frontiers | Frontiers in Marine Science

TYPE Original Research
PUBLISHED 10 January 2023
DOI 10.3389/fmars.2022.1050269

OPEN ACCESS

EDITED BY
Tommaso Tesi,
National Research Council (CNR), Italy

REVIEWED BY
Jerome Kaiser,
Leibniz Institute for Baltic Sea Research (LG), Germany
Kyung-Hoon Shin,
Hanyang University, South Korea

*CORRESPONDENCE
Yi Yang
yiyang@cug.edu.cn

SPECIALTY SECTION
This article was submitted to Marine Biogeochemistry, a section of the journal Frontiers in Marine Science

RECEIVED 21 September 2022
ACCEPTED 12 December 2022
PUBLISHED 10 January 2023

CITATION
Dong Z, Yang Y, Wang C, Bendle JA, Ruan X, Lü X and Xie S (2023) Development of a novel sea surface temperature proxy based on bacterial 3-hydroxy fatty acids. *Front. Mar. Sci.* 9:1050269. doi: 10.3389/fmars.2022.1050269

Development of a novel sea surface temperature proxy based on bacterial 3-hydroxy fatty acids

Zhengkun Dong[1], Yi Yang[1,2]*, Canfa Wang[1], James A. Bendle[3], Xiaoyan Ruan[4], Xiaoxia Lü[2] and Shucheng Xie[1]

[1]State Key Laboratory of Biogeology and Environmental Geology, Hubei Key Laboratory of Critical Zone Evolution, School of Earth Sciences, China University of Geosciences, Wuhan, China, [2]Hubei Key Laboratory of Marine Geological Resources, China University of Geosciences, Wuhan, China, [3]School of Geography, Earth and Environmental Sciences, University of Birmingham, Birmingham, United Kingdom, [4]Key Laboratory of Tectonics and Petroleum Resources of Ministry of Education, China University of Geosciences, Wuhan, China

Gram-negative bacterial 3-hydroxy fatty acids (3-OH-FAs) have received recent attention for their potential as palaeoclimate proxies. A novel temperature proxy, the ratio of *anteiso* to *normal* C_{13} 3-OH-FA (RAN_{13}), has been proposed for sea surface temperature (SST) reconstruction in the North Pacific Ocean. However, whether this newly proposed temperature proxy is applicable to marginal seas with significant terrigenous input or tropical oligotrophic seas requires further investigation. Here, we analyzed the composition and distribution of 3-OH-FAs and evaluated the possible impact of various environmental parameters (SST, water depth, dissolved oxygen, salinity and nutrient concentration) on their distribution in marine surface sediments from the Bohai Sea (BS) and the South China Sea (SCS). In the BS, the potential source proxy, fractional abundance of *anteiso* 3-OH-FAs (average 17%), indicates 3-OH-FA geochemical signature are not greatly overprinted by terrigenous inputs. The relative abundance of long-chain 3-OH-FAs (C_{15}-C_{18}) are higher in the SCS (average 41%) compared to those in other seas (average 33% for all marine samples). Massive inputs of terrigenous organic matter to the BS likely result in overestimation of SSTs based on the RAN_{13} proxy, and limited abundance of *anteiso* and *normal* C_{13} 3-OH-FAs in the oligotrophic SCS may increase the uncertainty of the RAN_{13} estimated SSTs. More importantly, we find that most short-chain 3-OH-FAs are temperature dependent, especially the fractional abundance of *i*-C_{12}, *a*-C_{13}, *i*-C_{14} and *n*-C_{14} with a high determination coefficient ($R^2 > 0.60$). Based on these newly found correlations, we propose a novel proxy: RANs. The RANs index shows a strong linear relationship with SST ($R^2 = 0.92$, $p < 0.001$, $n = 85$) and more accurate prediction than the RAN_{13}, especially in tropical samples. Furthermore, the RANs proxy is significantly correlated with TEX_{86}, and RANs-based SSTs are approximate to LDI derived temperature in the SCS, which support the reliability of RANs as a temperature proxy. These findings

further suggest 3-OH-FA based proxies have potential for paleo-SST reconstruction, especially at higher and lower ends of the ocean temperature spectrum and even in cases where marginal inputs of terrestrial organic matter and nutrients are high.

KEYWORDS

3-hydroxy fatty acids, temperature proxy, terrestrial input, Bohai Sea, South China Sea, sea surface temperature

1 Introduction

To better understand the climate system and provide context for future change, accurate reconstructions of past Sea Surface Temperatures (SSTs) is essential on various scales, from contemporary weather prediction to general circulation model simulations of past and future climates. Microbial lipid biomarkers have become key tools for paleoenvironment reconstruction due to their sensitive response to external environmental changes and high preservation rate (Eglinton and Eglinton, 2008). The preservation of a diverse array of lipid biomarkers in both ancient and modern marine sediments can be deployed for SST reconstruction. In the past few decades, three proxies, $U^{K'}_{37}$ (Brassell et al., 1986; Prahl and Wakeham, 1987), TEX_{86} (Schouten et al., 2002; Kim et al., 2008; Kim et al., 2010) and LDI (Rampen et al., 2012), based on C_{37} alkenones, glycerol dialkyl glycerol tetraethers (GDGTs), and long chain diols, respectively, have been proposed and widely used for paleo-SST reconstructions. Recently, Gram-negative bacterial derived lipid, 3-hydroxy fatty acids (3-OH-FAs), which were overlooked in the past, have been proposed as novel proxies (Wang et al., 2016, Yang et al., 2020a; Véquaud et al., 2021a; Wang et al., 2021a; Yang et al., 2021).

3-OH-FAs (carboxylic acids with a hydroxyl group in the third position), are derived from Gram-negative bacterial membranes. The lipid A of lipopolysaccharide (LPS), the main component of the outer membrane of Gram-negative bacteria, contains 3-OH-FAs with 10 to 18 carbon atoms (Wollenweber and Rietschel, 1990; Szponar et al., 2002; Szponar et al., 2003). 3-OH-FAs, which are bound to LPS by ester or amide bonds are well preserved in geological archives (Ten Haven et al., 1987; Wang et al., 2018; Yang et al., 2020a). To date, 3-OH-FAs have been found in a variety of environments, including fresh aerosols (Lee et al., 2004; Tyagi et al., 2015a), snow (Tyagi et al., 2015b; Tyagi et al., 2016), soils (Wang et al., 2016, Wang et al., 2021a; Yang et al., 2016; Huguet et al., 2019; Véquaud et al., 2021a; Véquaud et al., 2021b), speleothems (Wang et al., 2018), marine dissolved organic matter (DOM) and sediments (Wakeham et al., 2003; Yang et al., 2020a), lake sediments (Yang et al., 2021). More importantly, a series of novel proxies (e.g., RAN_{15}, RAN_{17}, RIAN etc.) based on empirical correlations of 3-OH-FAs were first proposed by Wang et al. (2016). These proxies were successfully applied to a Holocene stalagmite in reconstructing temperature and hydrological changes (Wang et al., 2018). More recently, different machine learning tools, based on the Gaussian Processes and Random Forests, have been applied to the fractional abundance of 3-OH-FAs in global soil datasets (Véquaud et al., 2021a; Wang et al., 2021a). These studies showed the wide applicability of those proxies and that machine learning approaches could improve accuracy and reduce Root Mean Square Error (RMSE). They also highlighted a distinct regionality of terrestrial 3-OH-FA distributions (possibly related to bacterial biogeographies) and suggested that no single global soil calibration is preferable to regional, local or context specific calibrations for terrestrial settings (Véquaud et al., 2021a; Wang et al., 2021a).

In the marine environment, 3-OH-FAs are abundant in both the water column and sediments (Wakeham, 1999; Wakeham et al., 2003). The correlation of the 3-OH-FA based proxies with satellite SSTs (Yang et al., 2020a) and the observation of the highest water column abundance of many Gram-negative bacterial groups and 3-OH-FAs in the upper water column (Wakeham, 1999) supports a predominantly upper water column origin (e.g., surface to deep chlorophyll maximum) for the marine sedimentary 3-OH-FA signal. Through comparisons of 16S rRNA gene sequences and 3-OH-FAs distributions between soil and marine sediments, Yang et al. (2020a) further proposed that the 3-OH-FAs in marine sediments are mainly derived from the water column. Furthermore, Yang et al. (2020a) found that soil-based proxies, RAN_{15} and RAN_{17}, were not applicable to the marine settings in the North Pacific Ocean. Instead, RAN_{13} (the ratio of *anteiso* to *normal* C_{13} 3-OH-FA) showed a significant exponential relationship with SST (R^2 = 0.92, $p< 0.001$, RMSE = 2.55, n = 45), and proposed it as a new paleothermometer.

Previous studies on biomarker based proxies (e.g., TEX_{86}, LDI) have found that terrestrial inputs could influence the microbial lipid-based temperature proxies, especially in coastal areas (Ohkouchi et al., 2002; Hopmans et al., 2004; de Bar et al., 2016). However, little is known about whether 3-OH-FA based

proxies are affected by significant terrigenous inputs. Yang et al. (2020a) also noted that the relationship between RAN_{13} and SST was weaker and large residual errors occurred in the high-temperature South China Sea (SCS), likely due to the low concentration of 3-OH-FAs in these regions. So, whether newly proposed 3-OH-FA based proxies can be used as a reliable paleo-thermometer needs further investigation. Here, we investigate the distribution of 3-OH-FAs in marine surface sediments from the Bohai Sea (BS) and the South China Sea, to further analyze the possible impact of environmental parameters on fractional abundance of 3-OH-FAs and to assess the performance of 3-OH-FA based temperature proxies in coastal seas with significant terrigenous inputs and warm marine regions.

2 Material and methods

2.1 Study area

The BS is a semi-closed coastal sea surrounded by the China mainland and the Liaodong Peninsula, with a surface area of 77 × 10^3 km^2 and an average depth of only 18 m (Figures 1A, B). The BS received large amounts of fresh water containing high nutrients and organic matters from the surrounded rivers like the Yellow River and the Haihe River over the last few decades (Chen, 2009), which caused a series of environmental and ecological crises.

The SCS is a tropical marginal sea with an area of 35 × 10^5 km^2 and an average depth of 1212 m. It connects with the Western Pacific Ocean through the 2200 m deep Luzon Strait between Taiwan Island and Luzon Island (Jia et al., 2012). Climatic variations of the SCS are primarily dominated by the East Asian Monsoon with annual SST ranging from 25 to 29°C (Figures 1A, C).

2.2 Sampling and environment parameters

We collected 25 surface sediments samples from the BS and the North Yellow Sea (Figure 1B) in 2018 and 15 surface sediments samples were collected from the SCS by the Guangzhou marine geological survey since 2005 (Figure 1C). All samples were stored at -20°C until lipid analysis. The annual and seasonal SST data for each sampling site were averaged over a 30-year period (1981-2010; NOAA dataset: http://www.esrl.noaa.gov/psd/). Other environmental parameter including water depth (WD), salinity, dissolved oxygen (DO) and nutrient concentration (nitrite, phosphate and silicate) were obtained as annual and seasonal averages from the WOA18 database with a 0.25° spatial resolution (https://odv.awi.de/en/data/ocean/world-ocean-atlas-2018/). We define the seasons as follows: Spring (March, April, and May); Summer (June, July, and August); Autumn (September, October, and November) and winter (December, January, February).

2.3 Lipid analysis

All marine sediments were freeze dried and ground to powder with a mortar and pestle prior before extraction. Samples (n = 40)

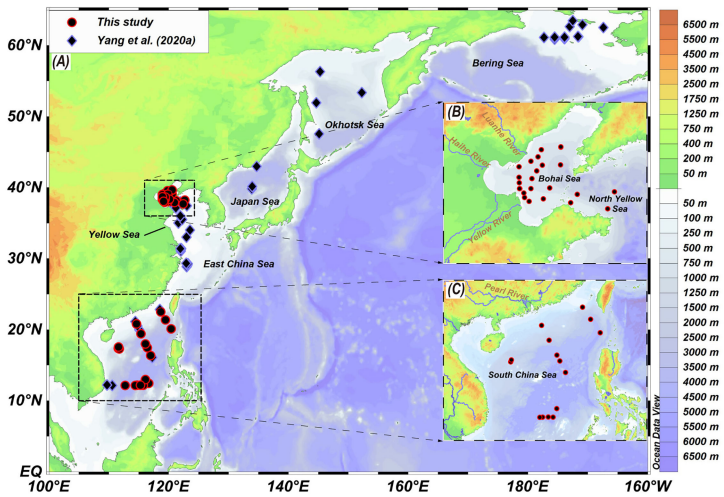

FIGURE 1
Maps showing the location in marine surface sediment samples. **(A)** Overview map in the North Pacific Sea showing all sampling sites (Yang et al., 2020a and this study). **(B, C)** Local maps showing the locations of surface sediment samples collected from the Bohai Sea and North Yellow Sea, and the South China Sea respectively.

were extracted using an optimized acid digestion method (Wang et al., 2012). First, about 10 g of homogenized sample was digested using 30 ml HCl (3 M) at 130°C for 3 h under a condensate reflux system. After cooling, the solutions were extracted 3 times by dichloromethane (DCM) through high-speed centrifuges, to obtain the total lipid extract (TLE). The TLE was condensed to 1-2 ml with a rotary evaporator and dried under gentle N_2. TLE was methylated in 2 ml BF_3-MeOH solution at 75°C for 1.5 h and extracted with *n*-hexane (× 5). The fatty acid methyl esters (FAMEs) were then separated into non-OH-FAMEs and OH-FAMEs using a silica gel column and eluting with a mixture solvent of *n*-hexane:ethyl acetate (98:2, v/v) and 100% ethyl acetate, respectively (Jenske and Vetter, 2008). The OH-FAME fraction was further derivatized with BSTFA (N, O-*bis* (trimethylsilyl) trifluoroacetamide) at 70°C for 1.5 h before analysis by gas chromatogram-mass spectrometer (GC-MS).

The 3-OH-FAs were analyzed by an Agilent 7890A gas chromatograph and a 5975C mass spectrometer equipped with a DB-5MS fused silica capillary column (60 m × 0.25 mm × 0.25 μm). The carrier gas was Helium (99.999% pure) and the gas flow was 1.0 ml·min^{-1}. The GC oven temperature was ramped from 70°C to 200°C at 10°C·min^{-1}, then to 310°C at 3°C·min^{-1}, held at 310°C for 30 min. The ionization energy of the mass spectrometer was set at 70 eV and the scan range was from 50 to 550 aum. The different 3-OH-FAs were identified based on their mass spectra and relative retention times. All the 3-OH-FAs TMSi esters show diagnostic fragment ions, m/z 175 ($[CH_3]_3SiO = CHCH_2CO_2CH_3)^+$, due to the cleavage between C3 and C4, and $M^+ = 15$ (base peak) results from a loss of a CH_3 group (Wang et al., 2016). The internal standard (androstane, 0.1 μg/μl) was co-injected with the derivatized 3-OH-FAs for quantification.

2.4 Statistical analysis and proxy calculations

We used Canoco 5 software to perform a redundancy analysis (RDA) to access the relationship of 3-OH-FA based proxies to environmental parameters including SST, WD, DO, oxygen and nutrient concentration, but not pH, since it shows a narrow variation and has a weak relationship with distribution of 3-OH-FAs in marine environments (Yang et al., 2020a). Origin 2022 software was employed to test the Pearson correlation coefficient among the 3-OH-FA fractional abundance and environmental parameters. A total of 85 samples were used for statistical analysis, including 40 samples from this study and 45 samples from Yang et al. (2020a).

3-OH-FA based proxies RAN_{13} and RIN_{17} (previously proposed as a proxy for lake mean annual air temperature) are calculated following Yang et al. (2020a) and Yang et al. (2021) respectively:

$$RAN_{13} = [anteiso\ C_{13}]/[normal\ C_{13}] \quad (1)$$

$$RIN_{17} = [iso\ C_{17}]/[normal\ C_{17}] \quad (2)$$

where *i*-, *a*- and *n*- represent *iso*, *anteiso*, and *normal* 3-OH-FA, respectively.

The quantitative correlation between SST and RAN_{13} is expressed in the following equation (Yang et al., 2020a):

$$SST = e^{3.75-0.47\times RAN_{13}} \quad (R^2 = 0.92,\ p < 0.001,\ RMSE = 2.55,\ n = 45) \quad (3)$$

3 Results

3.1 Environmental parameters

The mean annual SST in the BS and the SCS are in the range 12.6°C to 14.3°C and 25.9°C to 28.4°C (Supplementary Table S1), respectively. The seasonal SST ranges across the 85 sites (40 samples from this study and 45 samples from Yang et al. (2020a)) were as follows: spring: -1.0 to 28.9°C; summer: 6.3 to 29.3°C; autumn: 4.4 to 28.8°C; winter: -1.4 to 27.8°C. DO concentration (n = 85) varied from 182.48 μmol/kg to 337.60 μmol/kg with the highest value occurring in Bering Sea and the lowest value in the South China Sea. Salinity (n = 85) ranges from 30.02 to 34.63 psu. Nitrate, phosphate and silicate concentration (n = 85) are in the range 0.04 to 12.7 μmol/kg, 0.04 to 7.78 μmol/kg, 0.51 to 21.21 μmol/kg, respectively, without an evident spatial trend (Supplementary Table S1).

3.2 Concentration and composition of 3-OH-FAs in marine sediments

Data for all marine surface sediment samples (n = 85) were compiled (Figures 1A–C), including 40 new samples added in this study. The carbon numbers of 3-OH-FAs ranged from C_{10} to C_{18}, with even-numbered carbon compounds being more abundant than the odd-numbered ones (Figure 2). Concentrations of 3-OH-FAs ranged from 0.03 μg/g to 17.63 μg/g of dry sediment, with values for the BS (average 4.97 μg/g) being higher than the oligotrophic SCS (average 0.35 μg/g) (Supplementary Table S2). Even numbered 3-OH-FAs homologues were dominated by the C_{12}, C_{14}, C_{16} *normal* isomers with the *n*-C_{14} compound being the most abundant, whereas the C_{15} *anteiso* homologue was the highest peak of all

odd numbered compounds (Figure 2). Notably, unlike the even number homologues, the odd numbered C_{13}, C_{15} and C_{17} *normal* components were lower in relative abundance than their *anteiso* and *iso* isomers (Figure 2), with the exception of one sample from the SCS, where the *n*-C_{17} was more abundant. In addition, the unsaturated C_{18} 3-OH-FA was also detected (in line with results reported by Yang et al. (2020a); Figure 2).

The 3-OH-FA based SST proxy RAN_{13} was calculated following Eq. 1, with values ranging from 1.59 to 2.44 and from 0.37 to 1.87 in the BS and SCS, respectively. The RIN_{17} index was calculated using Eq. 2 with ranges from 0.23 to 5.01 and from 5.77 to 11.8 in the BS and SCS, respectively. The RIN_{17} values for 6 samples are missing because the *normal* C_{17} 3-OH-FA was below the detection limit in those samples (Supplementary Table S2).

3.3 Statistical analysis

To examine potential impact of environmental parameters on fractional abundance of 3-OH-FAs, Pearson Correlation Analysis was performed (Figure 3). Most of the short-chain 3-OH-FAs (C_{10}-C_{14}) show strong relationships with SST, WD, DO and salinity ($p< 0.05$; Figure 3), especially the *i*-C_{12}, *a*-C_{13}, *i*-C_{14} and *n*-C_{14} 3-OH-FAs with a coefficient of determination larger than 0.60 (Figure 4). In contrast, many long-chain 3-OH-FAs (C_{15}-C_{18}) show weak relationships with those environmental parameters. Environmental parameters including SST, WD, DO and salinity are also correlated with each other (Figure 3). Moreover, the RDA results show that annual mean SST explains most of the variability in 3-OH-FA based proxies (38.7%), while other parameters exert

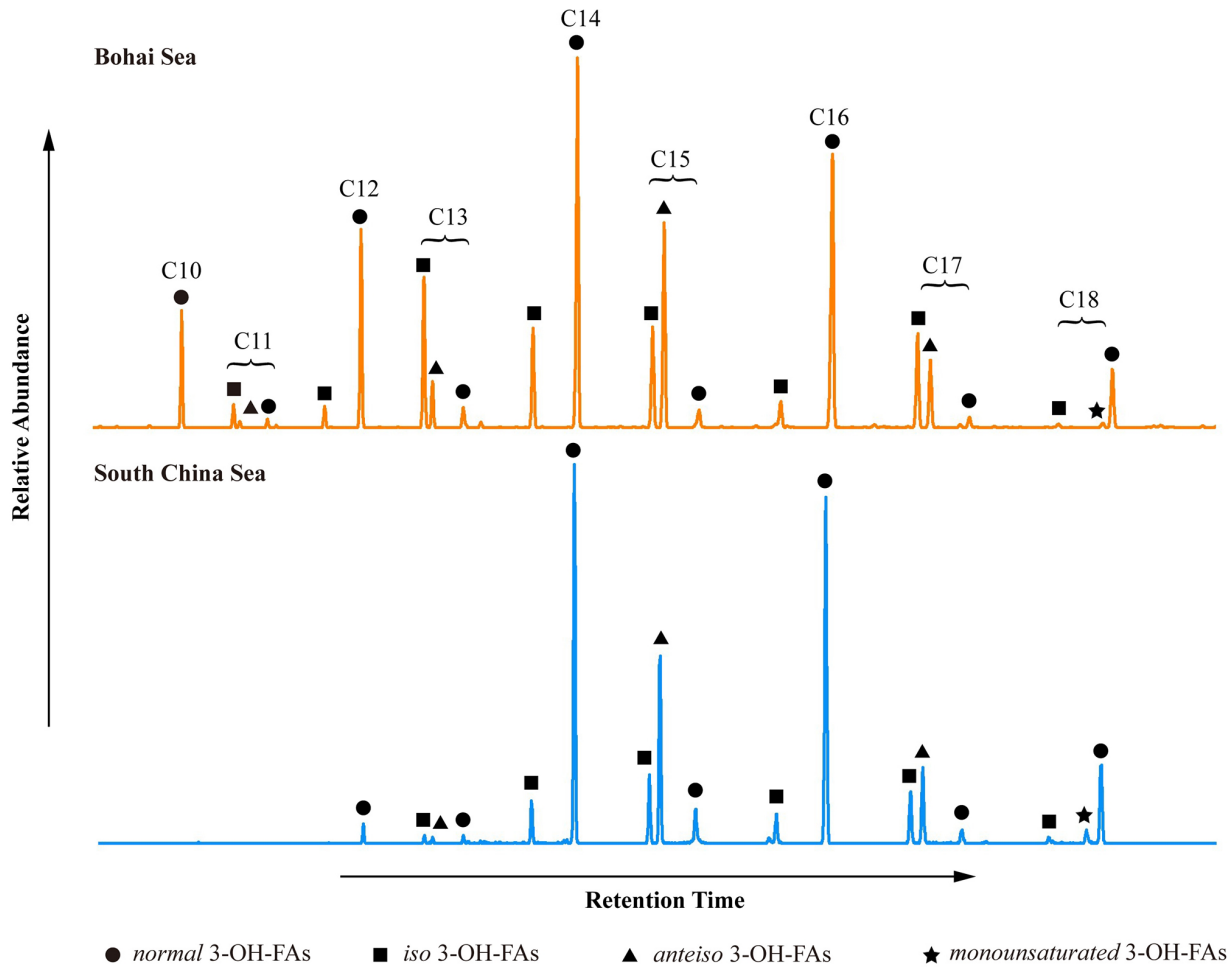

FIGURE 2
Examples showing typical distributions of 3-OH-FAs from the BS and SCS. The abundance of C_{10} and C_{11} 3-OH-FAs are below the detection limit and C_{13} 3-OH-FAs are low in samples from the SCS.

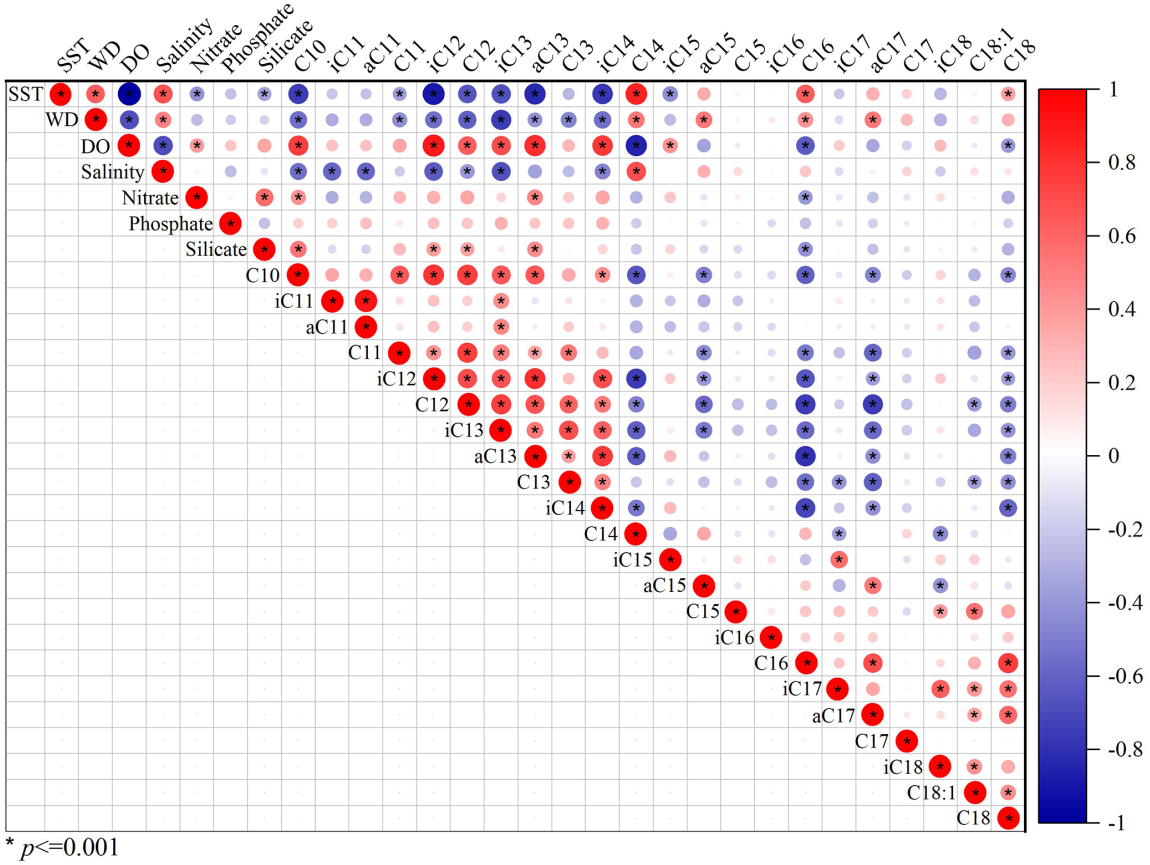

FIGURE 3
Hot map showing significant (p< 0.001) Pearson's correlation coefficients (circles) among the environmental parameters and fractional abundance of 3-OH-FAs (n = 81).

insignificant effect on these proxies (Figure 5). The RAN_{13} is significantly negatively correlated with SST, but RIN_{17} shows a weak relationship with temperature (Figure 5).

4 Discussion

4.1 Distribution of 3-OH-FAs in the BS and SCS

We use a ternary diagram to characterize 3-OH-FAs distributions in marine sediments, lake sediments and soil samples and find the distribution of 3-OH-FAs in the BS and SCS are consistent with the distribution reported by Yang et al. (2020a) (Figure 6). Generally, soil samples contain lower relative abundance of *anteiso* 3-OH-FAs compared to marine sediments and thus the fractional abundance of *anteiso* homologues in marine samples may have potential to assess the source of 3-OH-FAs, with higher values (ca. 13-30%) for predominant marine input and lower values (ca. < 13%) for terrestrial imprint (Figure 6). The ΣIIIa/ΣIIa ratio (branched glycerol dialkyl glycerol tetraethers (brGDGTs) based proxy) is generally< 0.59 in soils and 0.59–0.92 and > 0.92 in marine sediments with and without significant terrestrial inputs, respectively (Xiao et al., 2016). Both proxies were combined to investigate the distribution and source of 3-OH-FAs in the BS (Figures 7A, B).

A total of 33 samples including 25 from this study and 8 from Yang et al., 2020a in the BS show high abundance of *anteiso* 3-OH-FAs (> 13%), with the lowest value (13%) occurring near the Yellow River mouth (site B67) (Figure 7A). In addition, fractional abundance of *anteiso* 3-OH-FAs in the BS (average 17%) are close to those in all marine sample dataset (average 19%) and higher compared to the East China Sea, especially in Yangtze River estuary (Figure 7C). These characteristics suggest that although massive inputs of terrestrial materials into the BS by the Yellow River (Milliman and Meade, 1983), the influence of terrestrial contribution on 3-OH-FAs distribution is negligible except for samples close to river mouth. Notably, our results are consistent with the findings recorded by the ΣIIIa/ΣIIa ratio in the northern China Marginal Sea (Figures 7B, D). Liu et al.

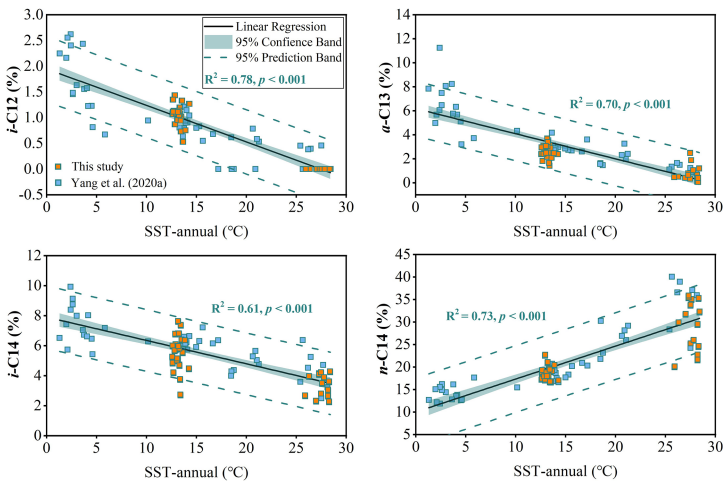

FIGURE 4
Cross plots showing the linear relationship between fractional abundance of 3-OH-FAs and annual mean SST.

(2021) reported that ∑IIIa/∑IIa have a higher average of 0.86 in the BS and lower average of 0.61 in the East China Sea and thus indicate that brGDGTs in most sediments of the BS are not overprinted by terrestrial inputs. The similar spatial distribution of these two indicators in the northern China Marginal Sea may be attributed to the fact that both 3-OH-FAs and brGDGTs are generally derived from bacteria.

In the SCS, fractional abundance of long-chain 3-OH-FAs (C_{15}-C_{18}) (average 41%, n = 15) is relatively higher than other seas (average 33% for all marine samples). The additional samples in this study contain relative higher abundance of $C_{15\text{-}18}$ 3-OH-FAs (ca. 25-60%, n = 15) compared to previous samples (ca. 25-40%, n = 7) (Yang et al., 2020a), especially in the central SCS (ca. 35-50%; Figure 6 and Supplementary Table S2). In fact, in the oligotrophic SCS, where total organic carbon (TOC) are lower than the BS, several short-chain homologues (C_{10} and C_{11}) are below the detection limit (Figure 2), resulting in the higher relative abundance of long-chain homologues in these samples.

4.2 Assessing the applicability of the RAN_{13} proxy to the BS and SCS

Numerous studies have shown that microbial lipid-based temperature proxies could be substantially biased by terrestrial inputs, especially in coastal areas (Ohkouchi et al., 2002; Hopmans et al., 2004; de Bar et al., 2016). The BS, which is subjected to massive terrestrial nutrient inputs from the Yellow River and the Haihe River (Milliman and Meade, 1983), could provide a test for the applicability of the 3-OH-FA based SST proxies in such conditions. The RAN_{13}-based residual SSTs (the temperature difference between observed and calculated value following Eq. 3) are less and little scattered in the BS except for one sample (site B67) with an extremely low RAN_{13} (1.59) (Figures 8A, B and Supplementary Table S2). We further analyze spatial distribution of RAN_{13} in the BS, and find that the abnormal low value is derived from the Yellow River mouth (Figure 7A), which may be partly biased by massive terrestrial organic matter inputs. In a word, the narrowed residuals suggest the RAN_{13} proxy has potential for tracing SST in the BS (Figure 8B). Notably, we find the RAN_{13}-based SSTs of most samples overestimate the observed SSTs in the BS (0.2-6.8°C) (Figure 8B). This overprediction may be attributed to two possibilities. Firstly, increases in microbially available carbon sources, due to massive terrestrial organic matter inputs, likely alter the microbial communities in the BS sediments including Gram-negative bacteria (Wang et al., 2021), the precursors of 3-OH-FAs. This hypothesis may be supported by the highest concentration of 3-OH-FAs observed in the BS (section 3.2; Yang et al., 2020a). Secondly, environmental crises, such as summer hypoxia, acidification and heavy metal pollution, may substantially influence the growth of Gram-negative bacteria (Wang et al., 2021), possibly resulting them to become less sensitive to temperature changes, however further study is needed to elucidate such a relationship.

Yang et al. (2020a) observed that RAN_{13} proxy had a weak relationship with SST and large residual errors in the warm SCS, which may be partly biased by the limited number of samples (n = 7) in these regions. Here we further test the applicability of the RAN_{13} to the tropical SCS with additional samples. Yet the residual errors of the RAN_{13} estimated SSTs appear large for tropical SSTs > 25°C (Figure 8B). As previously mentioned (section 4.1), the low TOC in the tropical

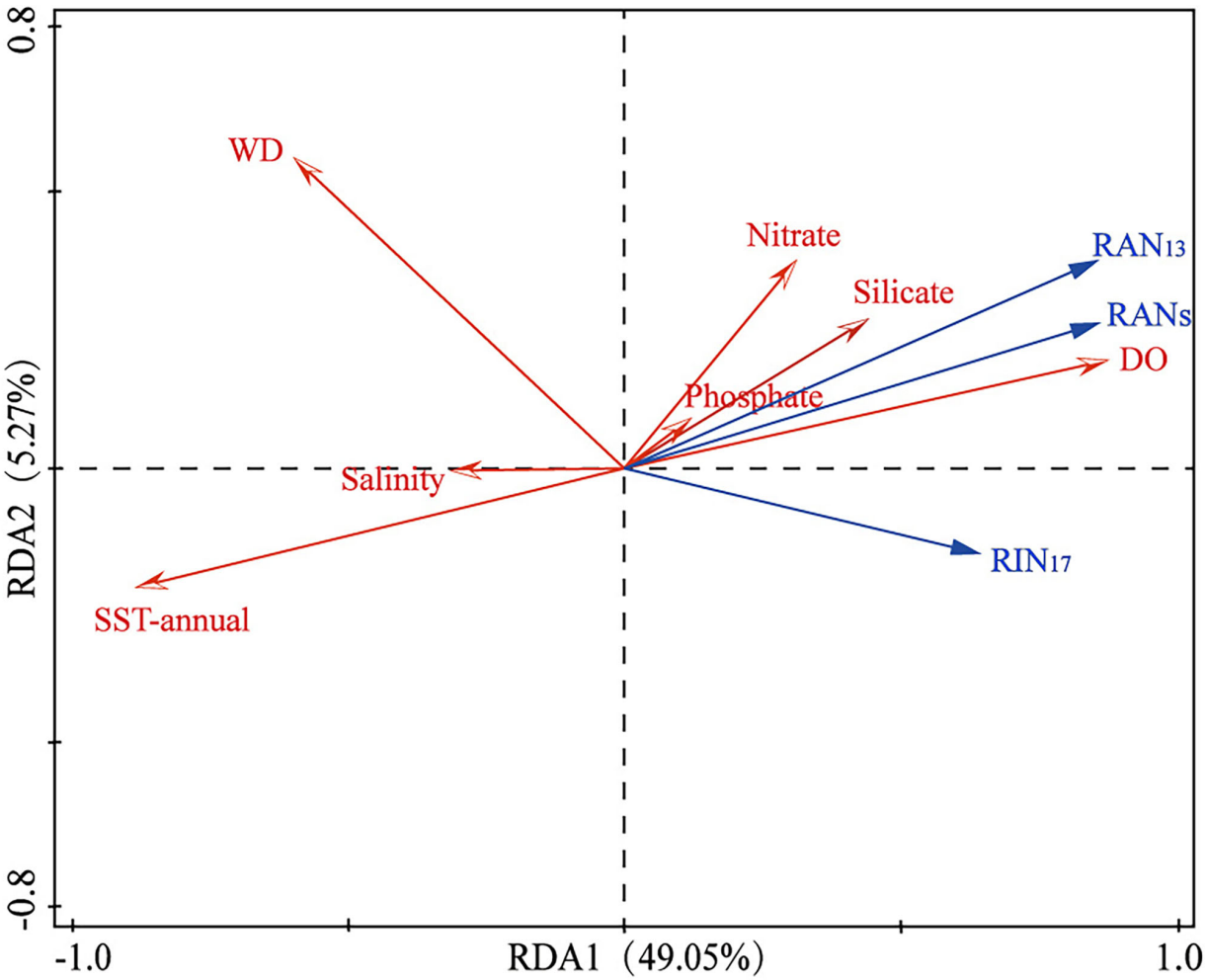

FIGURE 5
RDA biplot showing the relationship between environmental parameters and 3-OH-FA based proxies. The RDA1 explains 49.05% variation and RDA2 explains 5.27% variation (n = 77). WD, water depth; DO, dissolved oxygen concentration.

oligotrophic SCS may cause many homologues with low abundance falling below the detection limit. Also, the proxy associated homologues (*a*-C_{13} and *n*-C_{13}) maybe more inaccurate because of the limited abundance of these lipids, which increase prediction uncertainty in warm regions.

As discussed above, the limited abundance of *a*-C_{13} and *n*-C_{13} 3-OH-FAs due to low TOC may cause relatively large estimated errors in tropical oligotrophic SCS. Although analysts can inject merged samples to the GC-MS system, this is not an ideal solution as it decreases the temporal resolution for geological applications, especially for these geological archives with low TOC. Additionally, the RAN_{13}-based SST are higher than the measured SST in the BS. Furthermore, our RDA results indicate that lake-based temperature proxy RIN_{17} shows no significant relationship with SST in marine sediments (Figure 5), which may be attributable to different C_{17} 3-OH-FA producers in lake and marine settings as potentially supported by distinct distribution of 3-OH-FAs (Figure 6; Yang et al., 2021). Overall, the existing 3-OH-FA based temperature proxies (RAN_{13} and RIN_{17}) show relatively large uncertainties for SST reconstruction in tropical oligotrophic area and in the marginal sea with significant terrestrial inputs, which urges us to develop a new 3-OH-FA based proxy.

4.3 Appraisal of a novel proxy based on 3-OH-FAs for SST

Major environmental parameters such as temperature, salinity, DO and nutrients changes dramatically with latitude in the marginal seas of the North Pacific Ocean. Numerous studies have shown that these environmental parameters have

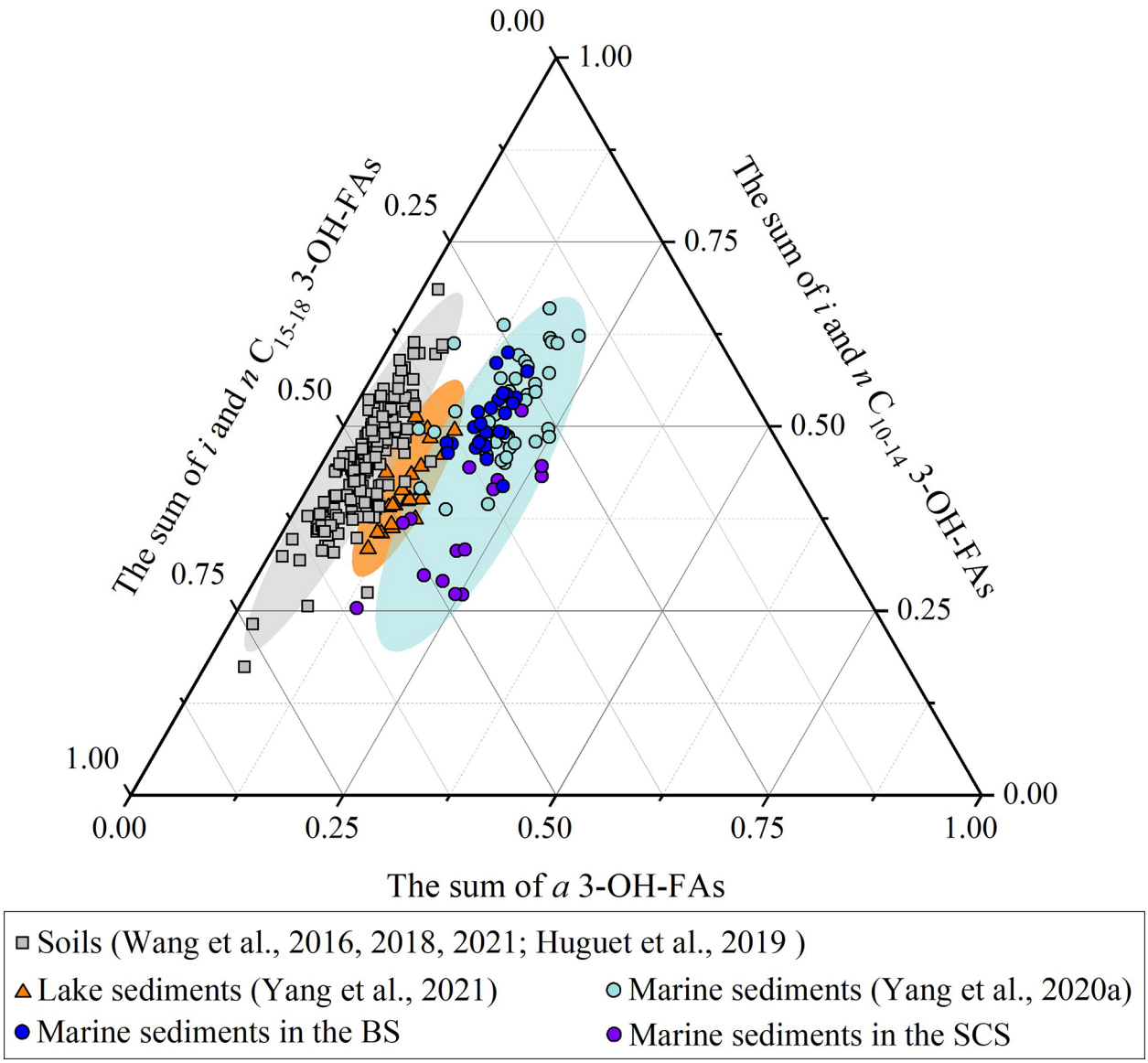

FIGURE 6
Ternary plot showing the relative abundance of 3-OH-FAs homologues in soils (Wang et al., 2016; Wang et al., 2018; Huguet et al., 2019, Wang et al., 2021a), lake surface sediments (Yang et al., 2021), marine surface sediments (Yang et al., 2020a and this study). The grey, orange, and blue ellipses show the main distribution area of soils, lake surface sediments and marine surface sediments distribution in the ternary plot, respectively.

potential to affect microbial and phytoplankton biomarker distribution (e.g., GDGTs, long chain diols) (Rampen et al., 2012; Lü et al., 2014). For example, elevated nutrient concentrations in summer could facilitate phytoplankton and Thaumarchaeotal growth to further affect the iGDGTs distribution in the east coastal sea of China (Lü et al., 2014). However, their effect on 3-OH-FAs distribution remains unclear. We thereby assess the potential impact of multiple environmental parameters on the fractional abundance of 3-OH-FAs with a Pearson Correlation Analysis by combining the previously published dataset (Yang et al., 2020a). The findings show that several 3-OH-FA homologues have a significant linear correlation with mean annual SST, DO and salinity (Figure 3). DO and salinity in surface seawater are partially controlled by temperature in the marginal seas of the North Pacific Ocean (Valjarević et al., 2020; Chen et al., 2022), since SST can affect seawater evaporation and gas solubility to further regulate DO and salinity, respectively (García and Gordon, 1992; Durack, 2015). Therefore, we conclude that temperature is a first order driver of 3-OH-FAs distribution in marine environments.

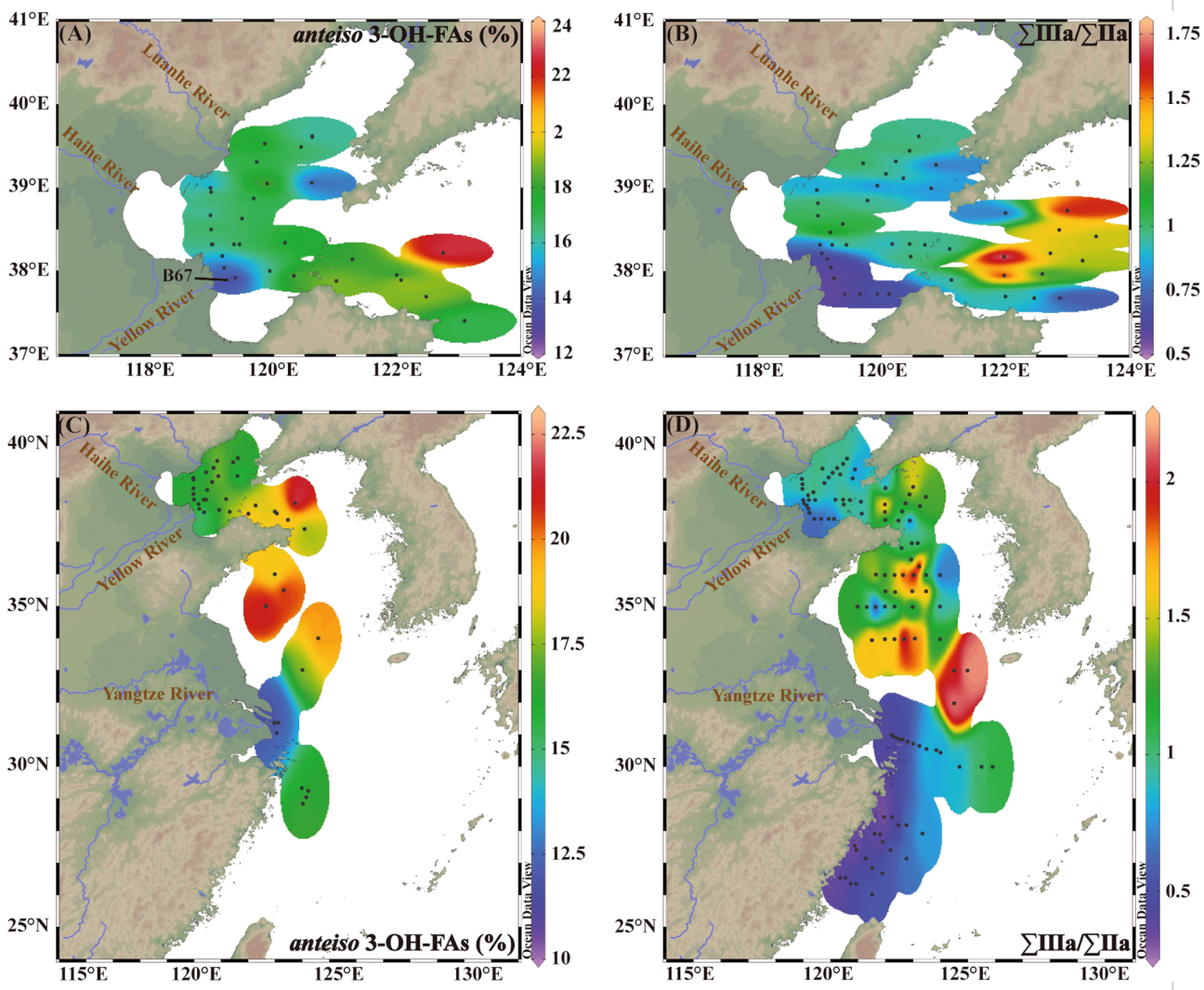

FIGURE 7
Spatial distributional patterns of fractional abundance of *anteiso* 3-OH-FAs (%) and ∑IIIa/∑IIa in the BS **(A, B)** and the northern China Marginal Sea **(C, D)**. 3-OH-FAs dataset **(A, C)** compiled from this study and Yang et al. (2020a). BrGDGTs dataset **(B, D)** are from Liu et al. (2021).

Notably, we find the majority of short-chain 3-OH-FAs (*n*-C_{10}, *i*-C_{12}, *n*-C_{12}, *i*-C_{13}, *a*-C_{13}, *i*-C_{14} and *n*-C_{14}) show a moderate or strong negative/positive correlation with temperature, whereas most long-chain homologues seem to be temperature independent (Figure 3). This may be explained by Yang et al. (2020a), which suggested short-chain 3-OH-FAs (C_{10}-C_{14}) may be generally produced by *in situ* bacteria from the marine water column, while the long-chain homologues (C_{15}-C_{18}) may have mixed sources with contribution from both *in situ* and terrestrial inputs.

Our empirical results strongly show that the fractional abundance of *i*-C_{12}, *a*-C_{13}, *i*-C_{14} and *n*-C_{14} 3-OH-FAs are controlled by temperature with the high determination coefficient among them ($R^2 > 0.60$, $p < 0.001$, n = 85; Figure 4). In other words, these evidently temperature dependent 3-OH-FAs may, in combination, be able to trace the temperature variation. Based on these findings, we add these temperature related short-chain homologues to the formula of the RAN_{13} to compute reasonable combinations (Supplementary Figure S1) and find the index which correlates best with SST (Figure 8C) is as follows:

$$RANs = (iC_{12} + aC_{13} + iC_{14})/(iC_{12} + aC_{13} + nC_{13} + iC_{14} + nC_{14}) \quad (4)$$

where s represents main short-chain homologues.

RDA results show the RANs index is positively related to SST (Table 1 and Figure 5), that it has a strong linear relationship (Figure 8C). Biomechanically, the common

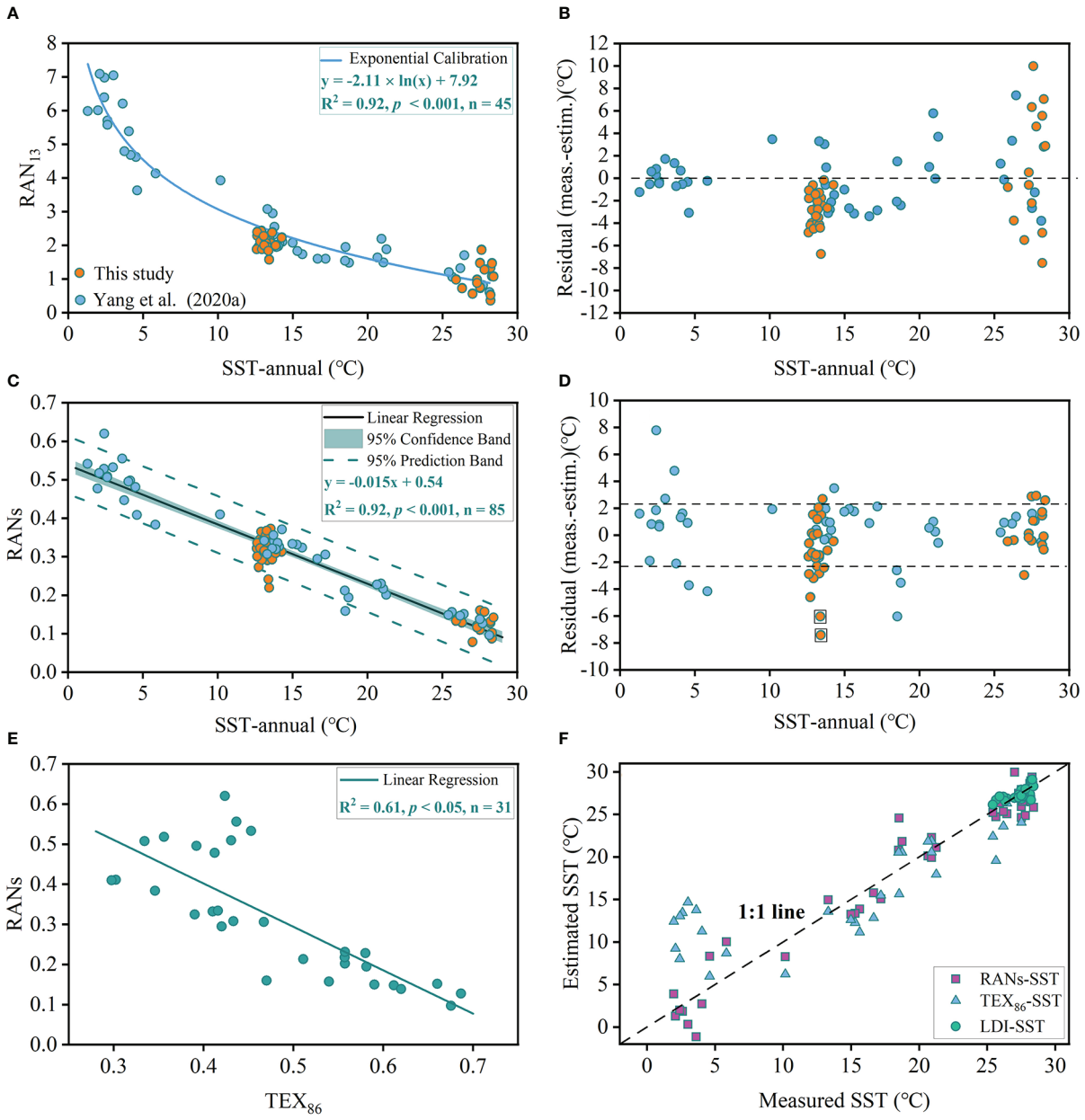

FIGURE 8
(A) Cross plot showing linear relationship between RAN_{13} and annual mean SSTs. The nonlinear regression equation is derived from Yang et al. (2020a) and the data used for fitting do not include 40 samples in this study. **(B)** The residual values between satellite and RAN_{13} estimated SSTs. **(C)** Cross plot showing linear relationship between RANs and annual mean SSTs. **(D)** The residual values between satellite and RANs estimated SSTs. Dashed lines denote the RMSE (2.3°C). Two samples in square frame are from the mouth of the Yellow River. **(E)** The linear relationship between RANs and TEX_{86}. **(F)** The relationship between the TEX_{86} derived SSTs, LDI derived SSTs and RANs-based SSTs compared with measured annual SSTs. TEX_{86} and LDI data are from Yang et al. (2020a) and Yang et al. (2020b), respectively.

principle of temperature response for existing 3-OH-FA based temperature proxies is that Gram-negative bacterial maintain proper membrane fluidity with temperature changes (Wang et al., 2016; Yang et al., 2020a; Yang et al., 2021), e.g. homeostasis of membrane lipid biophysical properties (Zhang and Rock, 2008). In fact, conversion of straight-chain fatty acids into branched chain fatty acids, induced at lower temperatures, likely proceeds since branched chain fatty acids help increase membrane fluidity (Denich et al., 2003). Membrane fluidity is closely related to phase transition temperature, the temperature at which a membrane shifts from the preferred liquid crystal phase into the gel

TABLE 1 Results of the RDA showing the contribution of environmental parameters to the variance of 3-OH-FA based proxies (RAN_{13}, RIN_{17} and RANs) in the marine sediments.

Order	Explanatory variable	Explains %	Contribution	*p*-Value
1	**SST-annual**	**38.7**	**71.3**	**0.002**
2	Salinity	4.6	8.5	0.012
3	WD	4.7	8.7	0.016
4	Nitrate	2.5	4.6	0.060
5	Silicate	2.1	3.8	0.062
6	DO	1.5	2.8	0.130
7	Phosphate	0.2	0.3	0.614

The bold values indicate SST explains most of the variability in 3-OH-FA based proxies.

phasewhen the temperature drops (Siliakus et al., 2017). Kaneda (1991) reported data from phase temperature experiments which utilized chemically synthesized acyl phosophatidylcholine and found that *iso*-C_{14} fatty acids hold a phase transition temperature of 6.5°C, which is 17.5°C lower than melting point for the *normal*-C_{14} alkyl fatty acids (24°C). This is highly relevant to the RANs index as the C_{14} 3-OH-FA is the most abundant homologue found in marine sediments. Kaneda (1991) found that the mean phase transition temperature was 19.7°C for the *iso* fatty acid isomers (C_{14} to C_{18}), 21°C lower that the average of 40.7°C for the *normal* isomers respectively. In addition, mean phase transition temperature was -4.4°C for C_{15} and C_{17} *anteiso* isomers, 45.1°C lower than the average (C_{14} to C_{18}) for the *normal* isomers. We suggest relationships for the C_{12} branched and normal isomers will follow a similar pattern as for the higher carbon number homologues, but no associated study has yet been reported.

Based on the linear relationship showed in Figure 8C, we obtain the following equation for annual SST calculation:

$$SST = -64.94 \times \mathrm{RANs} + 34.94\ (R^2 = 0.92, p < 0.001, RMSE = 2.29, n = 85) \quad (5)$$

The residual errors of the RANs estimated SST based on Eq. 5 are showed in Figure 8D, with a mean standard error of 2.29°C and most of the residuals fall within the error bar. In the BS, the overall estimated SSTs of RANs are closer to measured SSTs than these of RAN_{13} (Figures 8B, D), except for two samples near the mouth of Yellow River, whose geochemical signals have been heavily overprinted, as revealed by the highest BIT values (ca. 0.4) (Liu et al., 2021). Notably, the RANs proxy shows no correlation with temperature in soils or lake sediment samples for the available published data (Supplementary Figure S2) (Wang et al., 2016; Wang et al., 2018; Huguet et al., 2019; Véquaud et al., 2021a; Véquaud et al., 2021b; Wang et al., 2021a; Yang et al., 2021), whereas RAN_{13} provides a moderate correlation with MAAT (R^2 = 0.50, p< 0.05) in the lacustrine regimes (Yang et al., 2021). This is important as it suggests that RANs may be applied to marine archives without much concern that terrestrial inputs could overprint and greatly bias SST reconstruction. More importantly, estimated SSTs of RANs are more accurate compared to RAN_{13} in the tropical oligotrophic SCS (Figures 8B, D). This difference is apparently due to the fact that RANs proxy includes more temperature dependent homologues, which help to circumvent challenges associated with limited abundance of 3-OH-FAs in the SCS samples. In fact, the vast majority of low-latitude oceans around the globe are generally oligotrophic with low TOC, except for those near upwelling regions (Moore et al., 2013). Thus, it is crucial to develop such a temperature proxy for warm oceans. Meanwhile, we also note that the new calibration seems limited in the high-latitude oceans as residuals of RANs are relatively scatter in the Bering Sea (Figure 8D), and hereby should be utilized with great care. Overall, the better performance of the RANs calibration than the RAN_{13}, especially in the BS and warm SCS, suggests the new calibration is promising for reconstructing SST in the North Pacific Ocean.

To further assess the applicability of RANs proxy, we compared the RANs with other temperature proxies (TEX_{86} and LDI) in the same dataset (Yang et al., 2020a; Yang et al., 2020b). The results show strong linear relationship between RANs and TEX_{86} (R^2 = 0.61, p< 0.05, n = 31; Figure 8E), and the RANs-based temperature are closer to the measured SSTs (Figure 8F). Specifically, in the SCS, RANs-based SSTs are also approximate to local calibrated LDI-SSTs (Yang et al., 2020b; Figure 8F), supporting the reliability of RANs as a temperature proxy. Recently study revealed that the large scatter of TEX_{86}-based SSTs in the deep water might represent the winter seasonal bias of iGDGTs producer in the warm water (Jia et al., 2017). Therefore, it is of significance to analysis the seasonal difference of RANs proxy based on the dataset in this study. We hereby

investigate the relationship of both proxies with seasonal SST in the North Pacific marginal seas. The RAN_{13} proxy shows a strong correlation with SST for each season and all the determination coefficient values are > 0.64 (Supplementary Figure S3), but with highest correlations for summer and mean annual SSTs (R^2 = 0.91, p< 0.001, n = 85). The RANs index exhibits a strong relationship with all seasons (R^2 > 0.82, p< 0.001, n = 85) and the most robust relationship with summer SST (R^2 = 0.91, p< 0.001, n = 85; Supplementary Figure S4). This suggests that both proxies show slightly higher response to the warm seasonal SST in North Pacific marginal sea, probably resulting from the higher nutrient inputs from the surrounding large Rivers, like the Yangtze River and the Yellow River (Lü et al., 2014; Liu et al., 2021), during the warmer summer season. Although the RAN_{13} and RANs show higher relationship with warm seasonal SST, there are no significant seasonal difference for these two proxies (Supplementary Figures S3, S4), which might still represent the annual temperature change.

Furthermore, based on available 3-OH-FAs downcore data (Yang et al., 2020a), we reconstructed the annual mean SST based on different proxies (Figures 9A–D). RANs-based temperatures fluctuated from 16.5°C to 19.6°C (average 18.5°

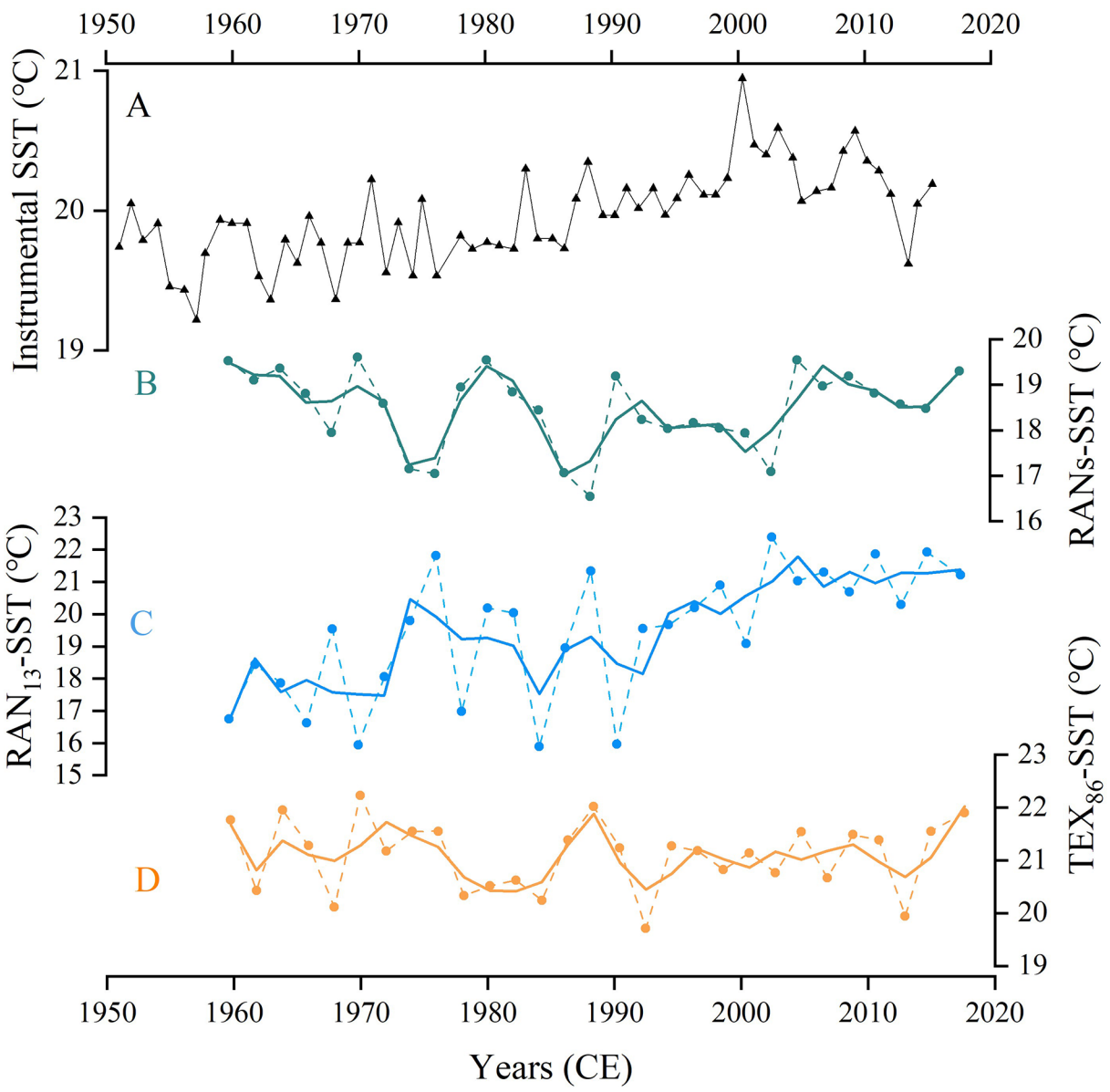

FIGURE 9
Comparison of RANs-SST record with other time-series and proxy records in in core B3. **(A)** Instrumental annual mean SST for core B3 (gridded from NOAA) since the 1950s. **(B)** and **(C)** showing RANs and RAN_{13} derived SSTs, respectively (data from Yang et al. (2020a)). **(D)** Annual mean SSTs derived from TEX_{86} (data from Lü et al. (2014)). The solid line represents 3 point moving average **(B–D)**.

C), during the past 58 years. Estimated SSTs based on RANs showed narrower variations and more stable fluctuations compared to these of RAN_{13}, which help to circumvent the over-sensitivity of RAN_{13} estimation (exponential calibration). Generally, the RANs-based SSTs varied from 1950CE to 1970CE, and showed increased trend thereafter. However, the temperature trends reconstructed based on RANs and RANs in core B3 showed slight differences, which might be attributed to multiple possibilities. The RAN_{13} depends on the factional abundance of *anteoiso* and *normal* C_{13}, whereas the RAN_{13} mainly relies on the distribution of C_{14} 3-OH-FA, which is accounts for about 30% among all 3-OH-FA homologues (Supplementary Table S2). As such, the distinct sensitivity or response pattern of C_{13} and C_{14} homologues to temperature changes may partly explain the differences of SST reconstruction. In fact, the TEX_{86}-based SSTs during the time period were not in good agreement with instrumental SSTs, which might indicate that the differences between RANs-SSTs and RAN_{13}-SSTs could be partially negligible just based on the short-term B3 core. However, previous studies have shown that TEX_{86} might not record SST but bottom water temperature (BWT), and low DO could greatly bias TEX_{86} estimation in the SCS (Wang et al., 2019; Guo et al., 2021). Therefore, undefined or non-thermal effects (such as, DO) may increase the uncertainty of RANs-SSTs, and the local or context specific calibrations seem preferable for downcore application.

The lack of information about microbial source of 3-OH-FAs in marine settings should indeed be taken into account while discussing the validity of the RANs proxy. Based on statistical analysis, we find the short-chain (C_{12}-C_{14}) 3-OH-FAs are temperature dependent in the North Pacific Ocean, but have no correlation with MAAT in the terrestrial environment (Wang et al., 2021a), which may be partly explained by the fact that these compounds are mainly from autochthonous marine bacteria (Yang et al., 2020a). Available genetic data revealed that 3-OH-FA producers in marine samples were mainly derived from alphaprotobacteria and gammaproteobacteria (Yang et al., 2020a), implying these Gram-negative bacteria might be as major contributions of C_{12}-C_{14} 3-OH-FAs in the investigated oceans. Modern water column analysis of 3-OH-FAs distribution and bacterial community analysis revealed that higher abundance of 3-OH-FAs and bacterial diversity in the euphotic zone (Wakeham, 1999; Brown et al., 2009). Therefore, the above evidences may reveal that C_{12}-C_{14} 3-OH-FAs in the sediments are mainly derived from Gram-negative bacteria dwelling in euphotic zone, with minor contribution of benthic organisms. However, more studies, such as, culture experiment of Gram-negative bacteria and carbon isotope analysis of 3-OH-FAs, are needed to constrain the source of individual 3-OH-FA compounds, and downcore applications are required to further test the reliability of RANs on geological time scales.

In summary, based on statistical analysis of 3-OH-FA fractional abundance in the BS and SCS and the published dataset in the Northern Pacific marginal sea, we found that most short-chain homologues were temperature dependent, and further proposed a novel 3-OH-FA based proxy (RANs) for SST. The RANs proxy showed certain advantages over RAN_{13}, especially in the warm/tropical oceans and the marginal seas with significant terrestrial inputs, and it was well-matched with other temperature proxies (TEX_{86} and LDI), indicating the potential of RANs for SST reconstruction.

5 Conclusions

Investigation of Gram-negative bacterial 3-OH-FAs in surface sediments from the BS and the SCS show that the distribution of these lipid is generally similar to previously reported. The relative abundance of *anteiso* 3-OH-FAs in the BS sediments shows that 3-OH-FAs may be mainly from autochthonous marine bacteria without significant terrestrial contribution. We find sediment samples from the oligotrophic SCS contain higher relative abundances of long-chain 3-OH-FAs (C_{15}-C_{18}) compared to other seas. We find that the RAN_{13} proxy overestimates the measured SST in the BS, and the residual SSTs are scattered and uncertainties are high in the SCS when using the RAN_{13} proxy. We also find that majority of short-chain 3-OH-FAs (*n*-C_{10}, *i*-C_{12}, *n*-C_{12}, *i*-C_{13}, *a*-C_{13}, *i*-C_{14} and *n*-C_{14}) are temperature dependent, especially the fractional abundance of *i*-C_{12}, *a*-C_{13}, *i*-C_{14} and *n*-C_{14}, with high determination coefficient. Based on these newly found correlations, we then propose a novel 3-OH-FA based temperature proxy: RANs. The RANs index exhibits a linear relationship with SST and more accurate estimation than RAN_{13}, especially when SST > 25°C. In addition, the RANs-based SSTs are consistent with existing temperature proxies (TEX_{86} and LDI) in the North Pacific Ocean, which indicates the potential of RANs as a new temperature proxy. Thus, our findings confirm the applicability of 3-OH-FA based proxies for marine SST estimation and we urge exploration of their application on geological timescales.

Data availability statement

The original contributions presented in the study are included in the article/Supplementary Material. Further inquiries can be directed to the corresponding author.

Author contributions

YY and CW contributed to conception and design of the study. ZD performed the experiments. ZD and YY analyzed the data and wrote the first draft of the manuscript. CW, JB, XR, XL, and SX edited and polished the manuscript. All authors contributed to the article and approved the submitted version.

Funding

This work was supported by the National Natural Science Foundation of China (No. 41821001, 41830319, 42203031), the 111 project (Program of Introducing Talents of Discipline to Universities; Grant No. BP0820004).

Acknowledgments

We thank Dr. Shu Yang and Prof. Weidong Zhai for providing the samples from the Bohai Sea. We sincerely thank Dr. Tommaso Tesi (Associate Editor) and two reviewers for their constructive suggestions for the manuscript.

Conflict of interest

The authors declare that the research was conducted in the absence of any commercial or financial relationships that could be construed as a potential conflict of interest.

Publisher's note

Supplementary material

The Supplementary Material for this article can be found online at: https://www.frontiersin.org/articles/10.3389/fmars.2022.1050269/full#supplementary-material

References

Brassell, S. C., Eglinton, G., Marlowe, I. T., Pflaumann, U., and Sarnthein, M. (1986). Molecular stratigraphy: A new tool for climatic assessment. *Nature* 320, 129–133. doi: 10.1038/320129a0

Brown, M. V., Philip, G. K., Bunge, J. A., Smith, M. C., Bissett, A., Lauro, F. M., et al. (2009). Microbial community structure in the north pacific ocean. *ISME J.* 3, 1374–1386. doi: 10.1038/ismej.2009.86

Chen, C.-T. A. (2009). Chemical and physical fronts in the bohai, yellow and East China seas. *J. Mar. Syst.* 78, 394–410. doi: 10.1016/j.jmarsys.2008.11.016

Chen, Y., Zhai, F., Gu, Y., Cao, J., Liu, C., Liu, X., et al. (2022). Seasonal variability in dissolved oxygen in the bohai Sea, China. *J. Ocean. Limnol.* 40, 78–92. doi: 10.1007/s00343-021-0235-6

de Bar, M. W., Dorhout, D. J. C., Hopmans, E. C., Rampen, S. W., Sinninghe Damsté, J. S., and Schouten, S. (2016). Constraints on the application of long chain diol proxies in the Iberian Atlantic margin. *Org. Geochem.* 101, 184–195. doi: 10.1016/j.orggeochem.2016.09.005

Denich, T. J., Beaudette, L. A., Lee, H., and Trevors, J. T. (2003). Effect of selected environmental and physico-chemical factors on bacterial cytoplasmic membranes. *J. Microbiol. Meth.* 52, 149–182. doi: 10.1016/S0167-7012(02)00155-0

Durack, P. J. (2015). Ocean salinity and the global water cycle. *Oceanography* 28, 20–31. doi: 10.5670/oceanog.2015.03

Eglinton, T. I., and Eglinton, G. (2008). Molecular proxies for paleoclimatology. *Earth Planet. Sci. Lett.* 275, 1–16. doi: 10.1016/j.epsl.2008.07.012

García, H. E., and Gordon, L. I. (1992). Oxygen solubility in seawater: Better fitting equations. *Limnol. Oceanogr.* 37, 1307–1312. doi: 10.4319/lo.1992.37.6.1307

Guo, J., Yuan, H., Song, J., Qu, B., Xing, J., Wang, Q., et al. (2021). Variation of isoprenoid GDGTs in the stratified marine water column: Implications for GDGT-based TEX_{86} paleothermometry. *Front. Mar. Sci.* 8. doi: 10.3389/fmars.2021.715708

Hopmans, E. C., Weijers, J. W. H., Schefuß, E., Herfort, L., Sinninghe Damsté, J. S., and Schouten, S. (2004). A novel proxy for terrestrial organic matter in sediments based on branched and isoprenoid tetraether lipids. *Earth Planet. Sci. Lett.* 224, 107–116. doi: 10.1016/j.epsl.2004.05.012

Huguet, A., Coffinet, S., Roussel, A., Gayraud, F., Anquetil, C., Bergonzini, L., et al. (2019). Evaluation of 3-hydroxy fatty acids as a pH and temperature proxy in soils from temperate and tropical altitudinal gradients. *Org. Geochem.* 129, 1–13. doi: 10.1016/j.orggeochem.2019.01.002

Jenske, R., and Vetter, W. (2008). Gas chromatography/electron-capture negative ion mass spectrometry for the quantitative determination of 2- and 3-hydroxy fatty acids in bovine milk fat. *J. Agric. Food Chem.* 56, 5500–5505. doi: 10.1021/jf800647w

Jia, G., Wang, X., Guo, W., and Dong, L. (2017). Seasonal distribution of archaeal lipids in surface water and its constraint on their sources and the TEX86 temperature proxy in sediments of the south China Sea. *J. Geophys. Res. Biogeosci.* 122 (3), 592–606. doi: 10.1002/2016JG003732

Jia, G., Zhang, J., Chen, J., Peng, P. A., and Zhang, C. L. (2012). Archaeal tetraether lipids record subsurface water temperature in the south China Sea. *Org. Geochem.* 50, 68–77. doi: 10.1016/j.orggeochem.2012.07.002

Kaneda, T. (1991). Iso- and anteiso-fatty acids in bacteria: Biosynthesis, function, and taxonomic significance. *Microbiol. Rev.* 55, 288–302. doi: 10.1128/MR.55.2.288-302.1991

Kim, J.-H., Schouten, S., Hopmans, E. C., Donner, B., and Sinninghe Damsté, J. S. (2008). Global sediment core-top calibration of the TEX_{86} paleothermometer in the ocean. *Geochim. Cosmochim. Acta* 72, 1154–1173. doi: 10.1016/j.gca.2007.12.010

Kim, J.-H., van der Meer, J., Schouten, S., Helmke, P., Willmott, V., Sangiorgi, F., et al. (2010). New indices and calibrations derived from the distribution of crenarchaeal isoprenoid tetraether lipids: Implications for past sea surface temperature reconstructions. *Geochim. Cosmochim. Acta* 74, 4639–4654. doi: 10.1016/j.gca.2010.05.027

Lee, A. K. Y., Chan, C. K., Fang, M., and Lau, A. P. S. (2004). The 3-hydroxy fatty acids as biomarkers for quantification and characterization of endotoxins and gram-negative bacteria in atmospheric aerosols in Hong Kong. *Atmos. Environ.* 38, 6307–6317. doi: 10.1016/j.atmosenv.2004.08.013

Liu, Y., Xiao, W., Wu, J., Han, L., Zhang, H., and Xu, Y. (2021). Source, composition, and distributional pattern of branched tetraethers in sediments of northern Chinese marginal seas. *Org. Geochem.* 157, 104244. doi: 10.1016/j.orggeochem.2021.104244

Lü, X. X., Yang, H., Song, J. M., Versteegh, G. J. M., Li, X. G., Yuan, H. M., et al. (2014). Sources and distribution of isoprenoid glycerol dialkyl glycerol tetraethers

(GDGTs) in sediments from the east coastal sea of China: application of GDGT-based paleothermometry to a shallow marginal sea. *Org. Geochem.* 75, 24–35. doi: 10.1016/j.orggeochem.2014.06.007

Milliman, J. D., and Meade, R. H. (1983). World-wide delivery of river sediment to the oceans. *J. Geol.* 91, 1–21. doi: 10.1086/628741

Moore, C. M., Mills, M. M., Arrigo, K. R., Berman-Frank, I., Bopp, L., Boyd, P. W., et al. (2013). Processes and patterns of oceanic nutrient limitation. *Nat. Geosci.* 6, 701–710. doi: 10.1038/ngeo1765

Ohkouchi, N., Eglinton, T. I., Keigwin, L. D., and Hayes, J. M. (2002). Spatial and temporal offsets between proxy records in a sediment drift. *Science* 298, 1224–1227. doi: 10.1126/science.1075287

Prahl, F. G., and Wakeham, S. G. (1987). Calibration of unsaturation patterns in long-chain ketone compositions for palaeotemperature assessment. *Nature* 330, 367–369. doi: 10.1038/330367a0

Rampen, S. W., Willmott, V., Kim, J.-H., Uliana, E., Mollenhauer, G., Schefuß, E., et al. (2012). Long chain 1,13- and 1,15-diols as a potential proxy for palaeotemperature reconstruction. *Geochem. Cosmochim. Acta* 84, 201–216. doi: 10.1016/j.gca.2012.01.024

Schouten, S., Hopmans, E. C., Schefuß, E., and Damste, J. S. S. (2002). Distributional variations in marine crenarchaeotal membrane lipids: A new tool for reconstructing ancient sea water temperatures? *Earth Planetary Sci. Lett.* 204, 265–274. doi: 10.1016/S0012-821X(02)00979-2

Siliakus, M. F., van der Oost, J., and Kengen, S. W. M. (2017). Adaptations of archaeal and bacterial membranes to variations in temperature, pH and pressure. *Extremophiles* 21, 651–670. doi: 10.1007/s00792-017-0939-x

Szponar, B., Krasínik, L., Hryniewiecki, T., Gamian, A., and Larsson, L. (2003). Distribution of 3-hydroxy fatty acids in tissues after intraperitoneal injection of endotoxin. *Clin. Chem.* 49, 1149–1153. doi: 10.1373/49.7.1149

Szponar, B., Norin, E., Midtvedt, T., and Larsson, L. (2002). Limitations in the use of 3-hydroxy fatty acid analysis to determine endotoxin in mammalian samples. *J. Microbiol. Meth.* 50, 283–289. doi: 10.1016/S0167-7012(02)00038-6

Ten Haven, H. L., Baas, M., De Leeuw, J. W., and Schenck, P. A. (1987). Late quaternary Mediterranean sapropels, I — on the origin of organic matter in sapropel S7. *Mar. Geol.* 75, 137–156. doi: 10.1016/0025-3227(87)90100-9

Tyagi, P., Ishimura, Y., and Kawamura, K. (2015a). Hydroxy fatty acids in marine aerosols as microbial tracers: 4-year study on β- and ω-hydroxy fatty acids from remote chichijima island in the western north pacific. *Atmos. Environ.* 115, 89–100. doi: 10.1016/j.atmosenv.2015.05.038

Tyagi, P., Kawamura, K., Bikkina, S., Mochizuki, T., and Aoki, K. (2016). Hydroxy fatty acids in snow pit samples from mount tateyama in central Japan: Implications for atmospheric transport of microorganisms and plant waxes associated with Asian dust. *J. Geophys. Res.: Atmos.* 121, 13641–13660. doi: 10.1002/2016JD025340

Tyagi, P., Kawamura, K., and Yamamoto, S. (2015b). Hydroxy fatty acids in fresh snow samples from northern Japan: long-range atmospheric transport of gram-negative bacteria by Asian winter monsoon. *Biogeosciences* 12, 7071–7080. doi: 10.5194/bg-12-7071-2015

Valjarević, A., Filipović, D., Milanović, M., and Valjarević, D. (2020). New updated world maps of sea-surface salinity. *Pure Appl. Geophys.* 177 (6), 2977–2992. doi: 10.1007/S00024-019-02404-z

Véquaud, P., Derenne, S., Anquetil, C., Collin, S., Poulenard, J., Sabatier, P., et al. (2021b). Influence of environmental parameters on the distribution of bacterial lipids in soils from the French Alps: Implications for paleo-reconstructions. *Org. Geochem.* 153, 104194. doi: 10.1016/j.orggeochem.2021.104194

Véquaud, P., Derenne, S., Thibault, A., Anquetil, C., Bonanomi, G., Collin, S., et al. (2021a). Development of global temperature and pH calibrations based on bacterial 3-hydroxy fatty acids in soils. *Biogeosciences* 18, 3937–3959. doi: 10.5194/bg-18-3937-2021

Wakeham, S. G. (1999). Monocarboxylic, dicarboxylic and hydroxy acids released by sequential treatments of suspended particles and sediments of the black Sea. *Org. Geochem.* 30, 1059–1074. doi: 10.1016/S0146-6380(99)00084-4

Wakeham, S. G., Pease, T. K., and Benner, R. (2003). Hydroxy fatty acids in marine dissolved organic matter as indicators of bacterial membrane material. *Org. Geochem.* 34, 857–868. doi: 10.1016/s0146-6380(02)00189-4

Wang, C. F., Bendle, J. A., Yang, H., Yang, Y., Hardman, A., Yamoah, A., et al. (2021a). Global calibration of novel 3-hydroxy fatty acid based temperature and pH proxies. *Geochem. Cosmochim. Acta* 302, 101–119. doi: 10.1016/j.gca.2021.03.010

Wang, C., Bendle, J. A., Yang, Y., Yang, H., Sun, H., Huang, J., et al. (2016). Impacts of pH and temperature on soil bacterial 3-hydroxy fatty acids: Development of novel terrestrial proxies. *Org. Geochem.* 94, 21–31. doi: 10.1016/j.orggeochem.2016.01.010

Wang, C., Bendle, J. A., Zhang, H., Yang, Y., Liu, D., Huang, J., et al. (2018). Holocene Temperature and hydrological changes reconstructed by bacterial 3-hydroxy fatty acids in a stalagmite from central China. *Quat. Sci. Rev.* 192, 97–105. doi: 10.1016/j.quascirev.2018.05.030

Wang, Y., Li, D.-W., Sachs, J. P., Hu, J., Cao, Y., Li, L., et al. (2019). Vertical distribution of isoprenoid GDGTs in suspended particles from the East China Sea shelf and implications for sedimentary TEX_{86}^{H} records. *Org. Geochem.* 136, 103895. doi: 10.1016/j.orggeochem.2019.07.004

Wang, C. X., Wang, Y., Liu, P., Sun, Y., Song, Z., and Hu, X. (2021b). Characteristics of bacterial community structure and function associated with nutrients and heavy metals in coastal aquaculture area. *Environ. pollut.* 275, 116639. doi: 10.1016/j.envpol.2021.116639

Wang, C., Zhang, H., Huang, X., Huang, J., and Xie, S. (2012). Optimization of acid digestion conditions on the extraction of fatty acids from stalagmites. *Front. Earth Sci.* 6, 109–114. doi: 10.1007/s11707-012-0311-5

Wollenweber, H.-W., and Rietschel, E. T. (1990). Analysis of lipopolysaccharide (lipid a) fatty acids. *J. Microbiol. Meth.* 11, 195–211. doi: 10.1016/0167-7012(90)90056-C

Xiao, W., Wang, Y., Zhou, S., Hu, L., Yang, H., and Xu, Y. (2016). Ubiquitous production of branched glycerol dialkyl glycerol tetraethers (brGDGTs) in global marine environments: A new source indicator for brGDGTs. *Biogeosciences* 13, 5883–5894. doi: 10.5194/bg-13-5883-2016

Yang, Y., Ruan, X., Gao, C., Lü, X., Yang, H., Li, X., et al. (2020b). Assessing the applicability of the long-chain diol (LDI) temperature proxy in the high-temperature south China Sea. *Org. Geochem.* 144, 104017. doi: 10.1016/j.orggeochem.2020.104017

Yang, Y., Wang, C., Bendle, J. A., Luo, Z., Dang, X., Xue, J., et al. (2021). Appraisal of paleoclimate indices based on bacterial 3-hydroxy fatty acids in 20 Chinese alkaline lakes. *Org. Geochem.* 160, 104277. doi: 10.1016/j.orggeochem.2021.104277

Yang, Y., Wang, C., Bendle, J. A., Yu, X., Gao, C., Lü, X., et al. (2020a). A new sea surface temperature proxy based on bacterial 3-hydroxy fatty acids. *Org. Geochem.* 141, 103975. doi: 10.1016/j.orggeochem.2020.103975

Yang, Y., Wang, C., Zhang, H., Huang, J., and Xie, S. (2016). Influence of extraction methods on the distribution pattern and concentration of fatty acids and hydroxy fatty acids in soil samples: Acid digestion versus saponification. *Geochem. J.* 50, 439–443. doi: 10.2343/geochemj.2.0422

Zhang, Y., and Rock, C. O. (2008). Membrane lipid homeostasis in bacteria. *Nat. Rev. Microbiol.* 6, 222–233. doi: 10.1038/nrmicro1839